Manganese (II) Coordination Complexes Involving Nitronyl Nitroxide Radicals

Mohammed Fettouhi,*,† Mazen Khaled,† Abdel Waheed,† Stéphane Golhen,‡ Lahcène Ouahab,*,‡ Jean-Pascal Sutter,§ and Olivier Kahn§

Chemistry Department, King Fahd University of Petroleum and Minerals, Dhahran 31261, Saudi Arabia, Laboratoire de Chimie du Solide et Inorganique Moléculaire, UMR 6511, Université de Rennes 1, Campus de Beaulieu, 35042, Rennes Cedex, France, and Laboratoire des Sciences Moléculaires, ICMCB, UPR CNRS no 9048, 33608 Pessac, France

Received March 11, 1999

Three new complexes involving nitronyl nitroxide and $PhCOO^-$ or N_3- ligands have been synthesized and structurally and magnetically characterized. These compounds are formulated as $Mn(L)_4(X)_2 \cdot nH_2O$, L = 2-(*p*-pyridyl)-4,4,5,5-tetramethylimidazoline-1-oxyl-3-oxide (PNN) or 2-(*p*-pyridyl)-4,4,5,5-tetramethylimidazoline-1-oxyl (PN) and X = $PhCOO^-$ or N_3^-. Compound **A** $[Mn(PNN)_2(PhCOO)_2(H_2O)_2]$ presents the following structural parameters: triclinic, space group $P\bar{1}$ (No. 2), $a = 6.859(1)$ Å, $b = 11.271(2)$ Å, $c = 13.978(6)$ Å, $\alpha = 88.88(2)°$, $\beta = 89.38(2)°$, $\gamma = 78.28(2)°$, $Z = 1$. The complex has a centrosymmetric distorted octahedral geometry in which the manganese ion is bound to two radical ligands through the nitrogen atom of the pyridine rings, two benzoate groups, and two water molecules. The two compounds **B** $[Mn(PNN)_4(N_3)_2]$ and **C** $[Mn(PN)_4(N_3)_2]$ are isostructural with the following structural parameters: **B**; triclinic, space group $P\bar{1}$ (No. 2), $a = 7.177(4)$ Å, $b = 13.767(3)$ Å, $c = 13.928(4)$ Å, $\alpha = 90.20(2)°$, $\beta = 102.94(4)°$, $\gamma = 91.86(4)°$, $Z = 1$; **C**, triclinic, space group $P\bar{1}$ (No. 2), $a = 7.004(2)$ Å, $b = 13.885(1)$ Å, $c = 14.036(2)$ Å, $\alpha = 90.34(1)°$, $\beta = 101.42(2)°$, $\gamma = 92.92(1)°$, $Z = 1$. They adopt a centrosymmetric tetragonally distorted octahedral geometry in which the manganese ion is bound to four radical ligands through the nitrogen atom of the pyridine rings, and the azido groups occupy the apical positions. For all three compounds **A**, **B**, and **C** intramolecular ferromagnetic interactions between the Mn(II) ion and the nitronyl nitroxide radicals are observed, but at very low temperatures, intermolecular antiferromagnetic interactions dominate.

Introduction

During the past two decades, the field of molecular magnets has attracted scientists from different horizons. Their main objectives are on one hand the chemical design of molecular assemblies that exhibit a spontaneous magnetization and on the other hand the rationalization of the magnetostructural correlations.[1]

Among the ligands capable of building extended 1D, 2D, and 3D networks in association with open-shell metal ions, great attention was devoted separately to both nitronyl nitroxides[2−4] and acetate, carboxylate, and azido anions.[1,5−15] Apart from the early solution ESR studies of some metal−pyridyl nitronyl nitroxide complexes, [16,17] the coordination chemistry of such ligands was initiated with the aim of building chainlike species. However, in most cases the NO groups of the radical do not coordinate even strongly electrophilic metal ions.[18,19] Meanwhile, the particular azido anion has emerged as a versatile ligand, generally leading to high-nuclearity systems with metals such as Mn(II),[5−12] Cu(II),[13,14]and Ni(II).[15] It stands furthermore as a good superexchange pathway, both antiferromagnetic in $\mu_{1,3}$-N_3 (end-to-end) coordination and ferromagnetic in $\mu_{1,1}$-N_3 (end-on) coordination. In the latter case ferromagnetic coupling has been interpreted by the spin polarization concept.[20] The most important examples of these systems are those exhibiting a spontaneous magnetization between 16 and 40 K.[5] The majority

† King Fahd University of Petroleum and Minerals.
‡ Université de Rennes 1.
§ ICMCB.

(1) Kahn, O. *Molecular Magnetism*; VCH: New York, 1993.
(2) Inoue, K.; Hayamizu, T.; Iwamura, H.; Hashizume, D.; Ohashi, Y. *J. Am. Chem. Soc*. **1996**, *118*, 1803.
(3) Caneschi, A.; Gatteschi, D.; Sessoli, R.; Rey, P. *Acc. Chem. Res*. **1989**, *22*, 392.
(4) Fegy, K.; Luneau, D.; Belorizky, E.; Novac, M.; Tholence, J. L.; Paulsen, C.; Ohm, T.; Rey, P. *Inorg. Chem.* **1998**, *37*, 4524.
(5) Escuer, A.; Vicente, R.; Goher, M. A. S.; Mautner, F. A. *Inorg. Chem.* **1997**, *36*, 3440.
(6) Escuer, A.; Vicente, R.; Goher, M. A. S.; Mautner, F. A. *Inorg. Chem*. **1998**, *37*, 782.
(7) Escuer, A.; Vicente, R.; Goher, M. A. S.; Mautner, F. A. *J. Chem. Soc., Dalton. Trans.* **1997**, 4431.
(8) Cortes, R.; Drillon, M.; Solans, X.; Lezama, L.; Rojo, T. *Inorg. Chem.* **1997**, *36*, 677.
(9) Escuer, A.; Vicente, R.; Goher, M. A. S.; Mautner, F. A. *Inorg. Chem*. **1996**, *35*, 6386.
(10) De Munno, G.; Julve, M.; Viau, G.; Lloret, F.; Faus, J.; Viterbo, D. *Angew. Chem., Int. Ed. Engl.* **1996**, *35*, 1807.
(11) Escuer, A.; Vicente, R.; Goher, M. A. S.; Mautner, F. A. *Inorg. Chem.* **1995**, *34*, 5707.
(12) Cortes, R.; Lezama, L.; Pizarro, J. L.; Arriortua, M. I.; Solans, X.; Rojo, T. *Angew. Chem., Int. Ed. Engl.* **1994**, *33*, 2488.
(13) Sikorav, S.; Bkouche-Waksman. I.; Kahn. O. *Inorg. Chem.* **1984**, *23*, 490.
(14) Agnus, Y.; Louis, R.; Gisselbrecht, J. P.; Weiss, R. *J. Am. Chem. Soc*. **1984**, *106*, 93.
(15) Ribas, J.; Monfort, M.; Ghosh, B. K.; Cortes, R.; Solans, X.; Font-Bardia, M. *Inorg. Chem.* **1996**, *35*, 864 and references therein.
(16) Richardson, P. F.; Kreilick, R. W. *J. Am. Chem. Soc*. **1977**, *99*, 8183.
(17) Richardson, P. F.; Kreilick, R. W. *J. Phys. Chem.* **1978**, *82*, 1149.
(18) Caneschi, A.; Ferraro, F.; Gatteschi, D.; Rey, P.; Sessoli, R. *Inorg. Chem.* **1990**, *29*, 4217.
(19) Luneau, D.; Risoan, G.; Rey, P.; Grand, A.; Caneschi, A.; Gatteschi, D.; Laugier, J. *Inorg. Chem.* **1993**, *32*, 5616.
(20) Charlot, M. F.; Kahn, O.; Chaillet, M.; Larrieu, C. *J. Am. Chem. Soc*. **1986**, *108*, 2574.

10.1021/ic9905751 CCC: $18.00
Published on Web 08/19/1999

of the polynuclear azido systems reported so far are pyridine-like or bipyridine adducts.[5−12] Therefore, in order to couple the two synthetic approaches, namely, realizing chainlike networks built with the azido ligand and metallic centers coordinated by spin- carrying ligands, we came up with the idea of using nitronyl nitroxide substituted pyridines. As a first approach the system Mn(II), N_3, PNN, or PN was investigated. Unlike the multicentercoordination schemes $\mu_{1,1}$ and $\mu_{1,3}$ adopted by the azido moieties in the 1D and 2D pyridine adducts, only mononuclear species were obtained.

Three new complexes have hence been isolated. We report herein the synthesis, X-ray structures, and magnetic characterizations of the three compounds **A** $[Mn(PNN)_2(PhCOO)_2(H_2O)_2]$, **B** $[Mn(PNN)_4(N_3)_2]$, and **C** $[Mn(PN)_4(N_3)_2]$, where PNN and PN stand for 2-(*p*-pyridyl)-4,4,5,5-tetramethylimidazoline-1-oxyl-3-oxide and 2-(*p*-pyridyl)-4,4,5,5-tetramethylimidazoline-1-oxyl, respectively.

Experimental Section

Syntheses. 2-(*p*-Pyridyl)-4,4,5,5-tetramethylimidazoline-1-oxyl-3-oxide and 2-(*p*-pyridyl)-4,4,5,5-tetramethylimidazoline-1-oxyl were prepared using literature procedures.[21]

Compound A. To a solution of manganese acetate tetrahydrate (2 mmol) and benzoic acid (4 mmol) in 40 mL of absolute ethanol was added a solid sample of PNN (4.3 mmol). The filtrate was kept in the dark for 1 week. Black crystals were then obtained.

Anal. Obsd (calcd) for $MnN_6C_{38}H_{46}O_{10}$: Mn, 6.7 (6.9); N, 10.76 (10.49); C, 57.15 (56.93); H, 5.96 (5.74). IR (KBr): 3455, 1615, 1541, 1395, 1330, 1225, 1145, 1083, 1029, 851, 729, 687 cm^{-1}.

Compound B. An aqueous solution of sodium azide (6 mmol) was added dropwise to a solution of manganese(II) chloride tetrahydrate (3 mmol) and PNN (12 mmol) in 50 mL of a (1/1) mixture of ethanol/water. The filtrate was allowed to stand for 3 days in the dark at room temperature. Black parallelepipedic crystals were obtained.

Anal. Obsd (calcd) for $MnN_{18}C_{48}H_{64}O_8$: Mn, 5.0 (5.1); N, 23.41 (23.44); C, 53.67 (53.58); H, 6.13 (5.95). IR (KBr): 2055, 1609, 1557, 1440, 1402, 1377, 1329, 1218, 1166, 1142, 1072, 1007, 831, 654 cm^{-1}.

Compound C. This compound was synthesized in a similar way as **B**, starting from PN instead of PNN. Shiny red crystals were hence obtained.

Anal. Obsd (calcd) for $MnN_{18}C_{48}H_{64}O_4$: Mn, 5.5 (5.4); N, 24.44 (24.92); C, 56.93 (56.96); H, 6.36 (6.32). IR (KBr): 2052, 1615, 1544, 1415, 1377, 1330, 1263, 1220, 1158, 1140, 1063, 1011, 842, 660 cm^{-1}.

Spectral and Magnetic Measurements. The IR spectra were measured on Perkin-Elmer spectrophotometer. Magnetic measurements were carried out using a Quantum Design SQUID SPMS-SS magnetometer working down to 2 K with magnetic fields up to 50 kOe. Data were corrected for the contribution of the sample holder, and diamagnetic contributions were estimated from Pascal's constants.

X-ray Data Collection and Structure Determination. Crystals were mounted on an Enraf-Nonius CAD4 diffractometer equipped with graphite-monochromatized Mo Kα radiation (λ = 0.710 73 Å). The unit cell parameters were obtained by least-squares fits of the automatically centered 25 reflections.

Intensity data were corrected for Lorentz and polarization effects. Data reduction and absorption correction using the ψ-scan method were performed with MolEN programs[22] and structure solution and refinements conducted with SHELXS-86 and SHELXL-97, respectively.[23,24] Crystallographic data are given in Table 1. Hydrogen atoms were found by Fourier syntheses or included at calculated positions with isotropic thermal parameters proportional to those of the connected carbon atoms.

Table 1. Crystallographic Data for **A**, **B** and **C**

	A	**B**	**C**
formula	$MnN_6C_{38}H_{46}O_{10}$	$MnN_{18}C_{48}H_{64}O_8$	$MnN_{18}C_{48}H_{64}O_4$
fw	801.75	1076.11	1012.11
cryst syst	triclinic	triclinic	triclinic
T (K)	293	293	293
λ (Å)	0.710 73	0.710 73	0.710 73
ρ_{calc} (g cm^{-1})	1.258	1.333	1.258
μ (mm^{-1})	0.371	0.315	0.306
a (Å)	6.859(1)	7.177(4)	7.004(2)
b (Å)	11.271(2)	13.767(3)	13.885(1)
c (Å)	13.978(6)	13.928(4)	14.036(2)
α (deg)	88.88(2)	90.20(2)	90.34(1)
β (deg)	89.38(2)	102.94(4)	101.42(2)
γ (deg)	78.28(2)	91.86(4)	92.92(1)
V ($Å^3$)	1057.9(5)	1340.4(9)	1336.0(4)
Z	1	1	1
R ($I_{obs} \geq 2\sigma(I)$)	0.0392(4118)	0.0418(4554)	0.0485(5291)
wR2	0.0898	0.1041	0.1225

[a] $R = \Sigma||F_o| - |F_c||/\Sigma|F_o|$ [b] $wR2 = \{\Sigma[w(F_o^2 - F_c^2)^2]/\Sigma[w(F_o^2)^2]\}^{1/2}$.

Selected bond lengths and angles are given in Table 2. Complete bond lengths and bond angles, anisotropic thermal parameters, and calculated hydrogen coordinates are deposited as Supporting Information. Figures 1, 2, and 3 give the ORTEP atomic labeling schemes for compounds **A**, **B**, and **C**, respectively.

Results and Discussion

Crystal Structures. The crystal structure of compound **A**, $[Mn(PNN)_2(PhCOO)_2(H_2O)_2]$, is displayed in Figure 4. The manganese ion lies on an inversion center and adopts a distorted octahedral coordination. Its coordination sphere is formed by two nitrogen atoms of the pyridyl groups, two carboxylic oxygen atoms, and two other oxygen atoms of the water molecules. The Mn−N bond length of 2.44(2) Å is somewhat longer than the corresponding one observed in compounds **B** and **C** described below. In the pyridyl nitronyl nitroxide ligand, the dihedral angle between the ON−C−NO fragment and the pyridyl ring is 24.7(1)°. The shortest intermolecular contact is observed in the *c* axis direction, between two nitronyl nitroxide groups of adjacent centrosymmetric $Mn(Ph_2)(PNN)_2(H_2O)_2$ units (O4···O4 = 3.77 Å). Intramolecular hydrogen bonding takes place between one oxygen atom of the carboxylic group and a hydrogen atom of the water molecule.

The molecular structures of compounds **B** $(Mn(PNN)_4(N_3)_2)$ and **C** $(Mn(PN)_4(N_3)_2)$, with the labeling schemes, are shown in Figures 2 and 3, respectively. These two compounds are isostructural. Similarly, the manganese ion lies on an inversion center and adopts a distorted octahedral coordination. It is bound to four nitrogen atoms of the pyridyl groups in addition to two azido ligands occupying the apical positions. The Mn−N (azido) bond distances are 2.198(2) and 2.160(2) Å for **B** and **C**, respectively, whereas the average Mn−N (pyridyl) bond distance is 2.322(2) Å. These values are close to those observed for other manganese complexes.[5−12] The N2−N1−Mn1 angles are 129.7(2)° and 126.5(2)° for compounds **B** and **C**, respectively. The dihedral angles between the NO−C−NO moieties and the pyridyl rings for the two independent PNN ligands are 34.8(1)° and 27.0(1)° for **B** and 31.7(1)° and 26.5(2)° for **C**, respectively, whereas the dihedral angles between the two adjacent NO−C−NO moieties of an asymmetric fragment are 74.3(2)° and 72.0(2)° for compounds **B** and **C**, respectively.

The crystal structures of **B** and **C** are displayed in Figures 5 and 6 as a projection on the *bc* plane.

For compound **B,** the shortest intermolecular contacts are established between the centrosymmetric oxygen atoms of the

(21) Ullman, E. F.; Call, L.; Osiecki, J. H. *J. Org. Chem.* **1970**, *35*, 3623.
(22) *Crystal Structure Analysis (MolEN)*; Enraf-Nonius: Delft, The Netherlands, 1990.
(23) Sheldrick, G. M. *SHELXS-86, Program for the solution of Crystal Structures*; University of Göttengen: Göttingen, Germany, 1985.
(24) Sheldrick, G. M. *SHELXL-93, Program for the refinement of Crystal Structures*; University of Göttingen: Göttingen, Germany, 1993.

Table 2. Selected Bond Lengths (Å) and Bond Angles (deg) for **A**, **B**, and **C**

A		**B**		**C**	
Mn1−O2	2.1363(12)	Mn1−N1	2.198(2)	Mn1−N1	2.1603(17)
Mn1−O1	2.2596(13)	Mn1−N4	2.3204(18)	Mn1−N7	2.3214(16)
Mn1−N1	2.4384(17)	Mn1−N7	2.3239(19)	Mn1−N4	2.3242(16)
O2−C1	1.258(2)	N1−N2	1.130(3)	N1−N2	1.182(2)
O3−C1	1.2635(19)	N2−N3	1.167(3)	N2−N3	1.146(3)
O4−N2	1.2761(17)	N7−C13	1.341(3)	N5−O1	1.258(3)
O5−N3	1.3205(19)	N7−C17	1.338(3)	N5−C6	1.390(3)
N1−C12	1.338(2)	O1−N9	1.267(2)	N5−C7	1.495(3)
N1−C8	1.416(2)	O2−N8	1.274(2)	N6−C6	1.284(3)
N3−C15	1.591(2)	N9−C18	1.342(3)	N6−C8	1.495(3)
N2−C14	1.566(2)	N9−C20	1.501(3)	N4−C1	1.335(2)
N3−C13	1.3533(19)	N8−C18	1.344(3)	N4−C5	1.342(2)
		N8−C19	1.510(3)	N8−O2	1.266(2)
		N4−C1	1.340(3)	N8−C18	1.388(3)
		N4−C5	1.342(3)	N8−C19	1.489(3)
		O3−N6	1.265(2)	N9−C18	1.282(3)
		O4−N5	1.273(2)	N9−C20	1.489(3)
		N6−C6	1.343(3)	N7−C13	1.332(2)
		N6−C8	1.495(3)	N7−C17	1.333(2)
		N5−C6	1.348(3)		
		N5−C7	1.508(3)		
O2−Mn1−O1	90.61(5)	N1−Mn1−N4	91.71(7)	N1−Mn1−N7	88.94(6)
O2−Mn1−N1	87.58(5)	N1−Mn1−N7	88.79(7)	N1−Mn1−N4	89.07(6)
O1−Mn1−N1	96.36(5)	N4−Mn1−N7	88.25(6)	N7−Mn1−N4	91.80(6)

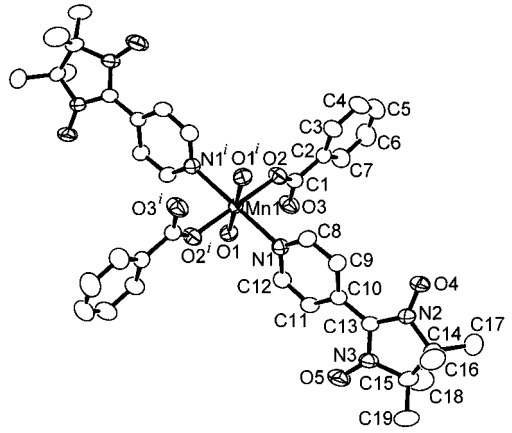

Figure 1. ORTEP view of the molecular structure of **A**. Thermal ellipsoids are drawn at the 50% probability level.

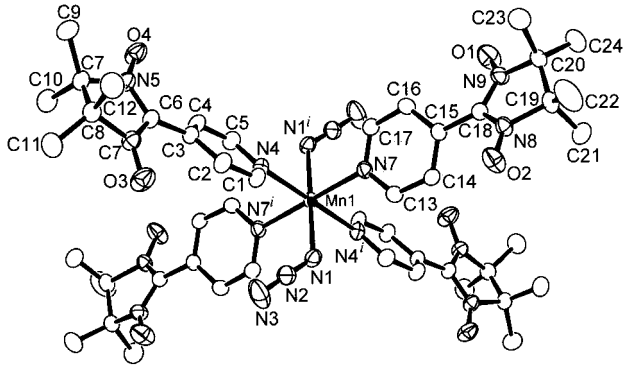

Figure 2. ORTEP view of the molecular structure of **B**. Thermal ellipsoids are drawn at the 50% probability level.

NO groups: O1···O1 (3.53 Å) and O4···O4 (3.60 Å). Such a contact scheme has a 2D (parallel *bc* plane) character ensured by the centrosymmetric parallel ON−C−NO fragments. However, for compound **C**, only a short 1D contact scheme is observed through centrosymmetric nitronyl groups (O1···O1: 3.77 Å) in the *c* axis direction.

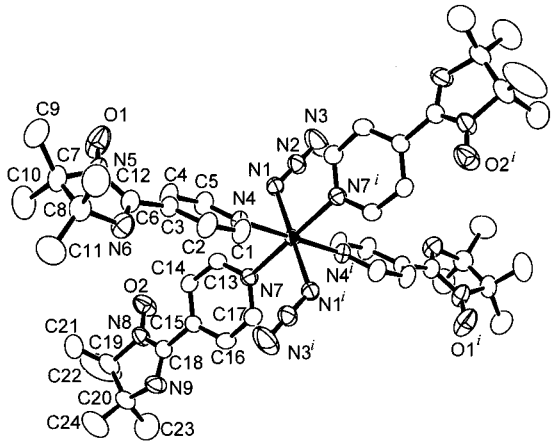

Figure 3. ORTEP view of the molecular structure of **C**. Thermal ellipsoids are drawn at the 50% probability level.

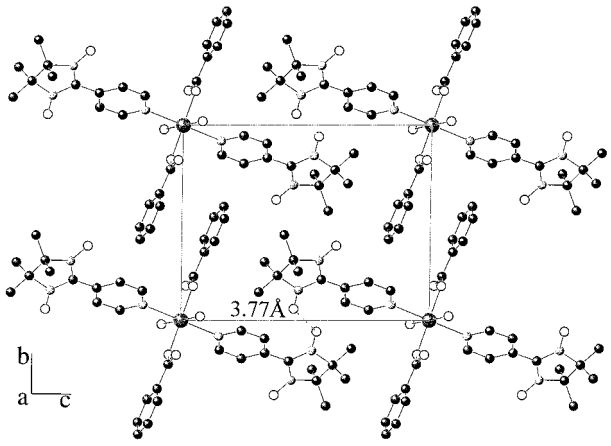

Figure 4. View of the structure of **A** in the *bc* plane.

Magnetic Properties. The temperature dependences of the magnetic susceptibility for compounds **A**−**C** were measured in the temperature range 2−300 K, with an applied field of 1000 Oe. The plots of $\chi_M T$ versus T, where χ_M is the molar magnetic susceptibility corrected for the core diamagnetism and T the

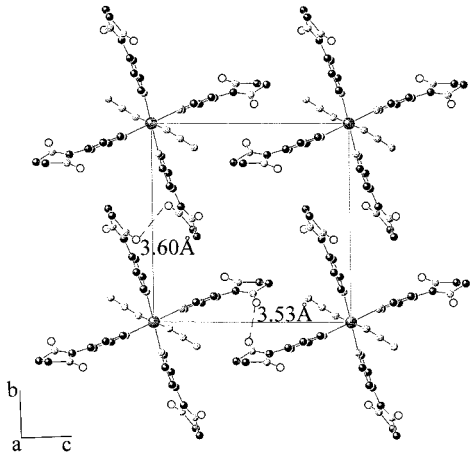

Figure 5. View of the structure of **B** in the *bc* plane.

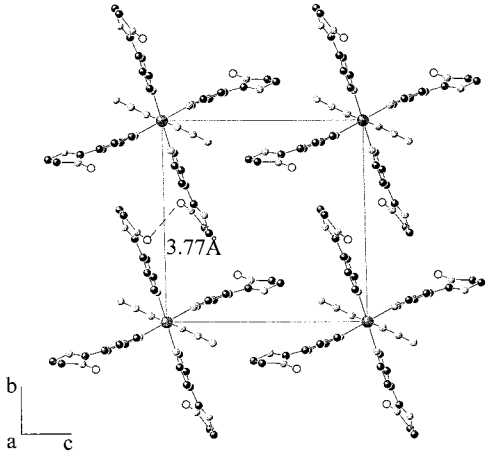

Figure 6. View of the structure of **C** in the *bc* plane.

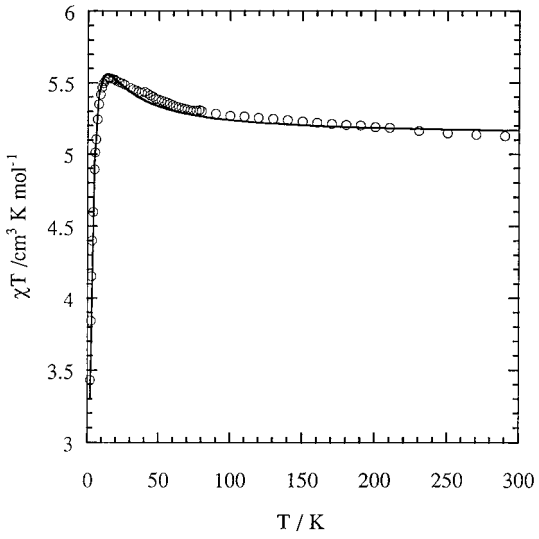

Figure 7. Temperature dependence of $\chi_M T$ for complex **A**.

temperature, are shown in Figures 7, 8, and 9 for compounds **A**, **B**, and **C**, respectively.

For $Mn(PNN)_2(PhCOO)_2(H_2O)_2$, **A**, the room temperature $\chi_M T$ value is approximately equal to 5.12 cm^3 K mol^{-1}, the expected value for the isolated $S_{Mn} = {}^5/_2$ and two $S_{rad} = {}^1/_2$ spins. As the temperature is lowered, $\chi_M T$ increases to reach a maximum of 5.6 cm^3 K mol^{-1} at 15 K and then decreases rapidly to about 3.4 cm^3 K mol^{-1} at 2 K (Figure 7). The profile of the curve is consistent with ferromagnetic interactions

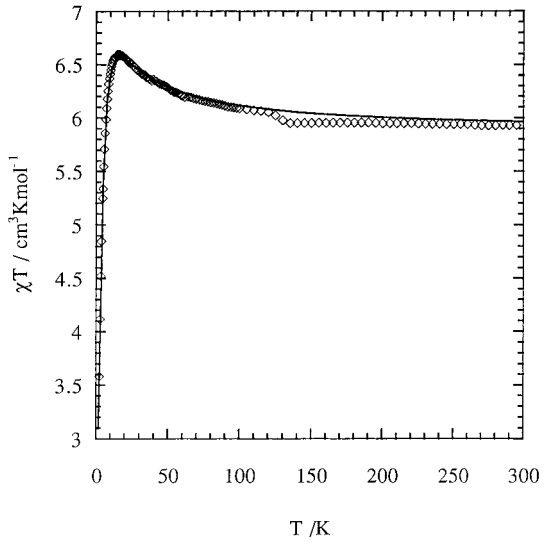

Figure 8. Temperature dependence of $\chi_M T$ for complex **B**.

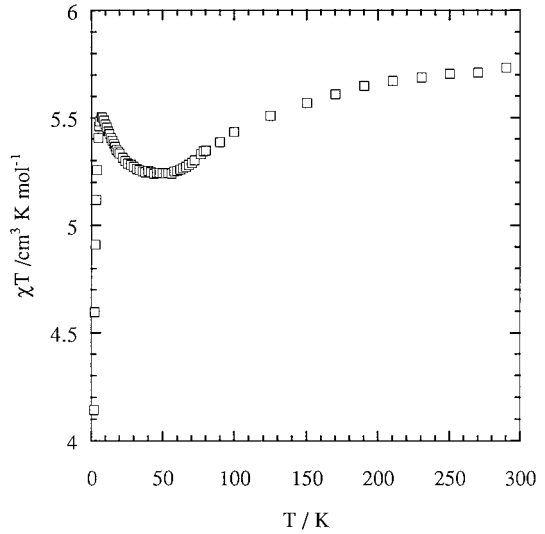

Figure 9. Temperature dependence of $\chi_M T$ for complex **C**.

attributed to the intramolecular Mn−radical interaction as observed in similar compounds.[25,26] The decrease of $\chi_M T$ below 15 K indicates the occurrence of intermolecular antiferromagnetic interactions which may result from the rather close proximity of the NO moieties of neighboring molecules (O4···O4′, 3.77 Å), as revealed by the X-ray structure analysis. Therefore the temperature dependence of the magnetic susceptibility was modeled with an expression of χ_M taking into account the intramolecular interaction between the Mn(II) ion and the two paramagnetic ligands, a theoretical expression deduced from the spin Hamiltonian $H = -J(S_{Mn}S_{rad1} + S_{Mn}S_{rad2})$. To take into account the decrease of $\chi_M T$ below 15 K, a weak intermolecular interaction based on the mean-field approximation, zJ', was introduced. Least-squares fitting of the experimental data led to $J = 3.1$ cm^{-1} and $zJ' = -0.3$ cm^{-1} (g_{Mn} and g_{rad} were taken equal to 2.00).

The temperature dependence of the magnetic susceptibility for $Mn(PNN)_4(N_3)_2$, **B**, is shown in Figure 8. At high temperature (150−300 K), $\chi_M T$ corresponds to the expected value, 5.9

(25) Chen, Z. N.; Qiu, J.; Gu, J. M.; Wu, M. F.; Tang, W. X. *Inorg. Chim. Acta* **1995**, *233*, 131−5.
(26) Caneschi, A.; Ferraro, F.; Gatteschi D.; Rey, P.; Sessoli, R. *Inorg. Chem.* **1990**, *29*, 4217.

cm^3 K mol^{-1}, for the uncorrelated spins of the Mn(II) and the nitronyl nitroxides. As the temperature is lowered from 150 to 2 K, $\chi_M T$ first increases to reach a maximum of 6.6 cm^3 K mol^{-1} at 18 K and then decreases rapidly to about 3.6 cm^3 K mol^{-1} at 2 K. As for compound **A**, the profile of this curve indicates the coexistence of ferromagnetic and weaker antiferromagnetic interactions. This behavior is well reproduced by a spin Hamiltonian taking into account both Mn−radical, J, and radical−radical, J', intramolecular magnetic interactions (eq 1), the intermolecular interactions being considered in the mean-field approximation as zJ''. However, considering the distances between the nitronyl nitroxide units within a molecule, no significant radical−radical magnetic interaction is expected so that J' was fixed to zero. Least-squares fitting of the experimental data led to $J = 4.7$ cm^{-1}, $J' = 0$ (fixed)[27] and $zJ' = -0.5$ cm^{-1} (g_{Mn} and g_{rad} were taken equal to 2.00). These results are in good agreement with the magnetic interactions found in compound **A** and compounds described in the literature,[25,26] confirming the ferromagnetic nature of the magnetic interaction between the Mn(II) ion and the nitronyl nitroxide radical through the *p*-pyridyl moiety.

$$H = -JS_{Mn}(S_{rad1} + S_{rad2} + S_{rad3} + S_{rad4}) - J'(S_{rad1}S_{rad2} + S_{rad2}S_{rad3} + S_{rad3}S_{rad4} + S_{rad4}S_{rad1}) \quad (1)$$

Despite the structural similarity between **B** and **C**, their magnetic behavior is quite different. The temperature dependence of the magnetic susceptibility for compound **C** is shown in Figure 9 in the form of the variation of $\chi_M T$ versus T. At high temperature $\chi_M T$ of **C** is slightly below the expected value of 5.9 cm^3 K mol^{-1}. As the temperature is lowered, $\chi_M T$ decreases slowly to reach near 50 K a kind of plateau at ca. 5.2 cm^3 K mol^{-1}. Then, it increases again to reach a maximum of 5.5 cm^3 K mol^{-1} at 7 K before dropping to 4.1 cm^3 K mol^{-1} at 2 K. Compared to **A** and **B**, there is clearly a rather strong antiferromagnetic interaction occurring in compound **C**. It is likely to be the result of the interaction between two of the nitronyl groups of **C** with one radical unit of two neighboring complexes. This is supported by the X-ray analysis. In fact, two of the four radicals of a molecule have been found to be close to that of two neighboring molecules. The NO centers are nearly parallel to each other with N···O distances of 3.71 and 3.77 Å, an ideal position for the overlap of the p orbitals forming thus a pair of radicals with a substantial antiferromagnetic interaction. It can be noticed that the plateau reached by the curve between 50 and 30 K corresponds approximately to the expected $\chi_M T$ value for the uncorrelated spins $S_{Mn} = {}^5/_2$ and two $S_{rad} = {}^1/_2$ spins. This confirms that the magnetic moments of two radical units of the molecule have been canceled by the intermolecular antiferromagnetic interactions. Below 30 K the intramolecular ferromagnetic interactions between the Mn(II) ion and its paramagnetic ligands start to take place, hence increasing the global moment of the molecule. The consequence is an increase of $\chi_M T$ value, which however drops rapidly as soon as the ferromagnetic cluster corresponding to the molecule orders antiferromagnetically with its neighboring clusters via the radical−radical interaction, leading normally to a nonmagnetic ground state. The high-temperature (300−50 K) decrease of $\chi_M T$ can be well reproduced by a pair model of $S = {}^1/_2$ spins to yield an exchange parameter $J = -130$ cm^{-1}. Related rather strong through-space antiferromagnetic interactions between aminoxyl radicals have been described recently.[28]

For compound **B**, the anomaly observed in the $\chi_M T$ plot at around 130 K suggests the occurrence of a structural transition.

Concluding Remarks

Unlike the high nuclearity of the systems of formula $Mn^{II}(L)_m(N_3)_n$ (L = pyridine-like ligand) reported so far, only mononuclear species were obtained when the ligand L was PNN or PN. These results raise once again the ambiguity of the subtle factors governing the coordination mode of the azido moiety and the influence of the ligand L. From the magnetic point of view, the *p*-pyridine moiety behaves as an intramolecular ferromagnetic pathway between the Mn(II) and the nitronyl centers as found in similar magnetic clusters while antiferromagnetic intercluster interactions dominate at low temperature. Such magnetic interactions are related to the encountered molecular packing schemes allowing significant overlap between adjacent molecular magnetic orbitals.

Acknowledgment. Support from King Fahd University of Petroleum and Minerals, Saudi Arabia, is gratefully acknowledged.

Supporting Information Available: Three X-ray crystallographic files, in CIF format. This material is available free of charge via the Internet at http://pubs.acs.org.

IC9905751

(27) Least-squares fitting of the experimental data with all three contributions led to $J = 4.5$ cm^{-1}, $J' = 2$ cm^{-1}, and $zJ' = -0.5$ cm^{-1}.

(28) Akabane, R.; Tanaka, M.; Matsuo, K.; Koga, N.; Matsuda, K.; Iwamura, H. *J. Org. Chem.* **1997**, *62*, 8854. Ishimaru, Y.; Kitano, M.; Kumada, H.; Koga, N.; Iwamura, H. *Inorg. Chem.* **1998**, *37*, 2273.